Conformational Analysis of β-1,2-Linked Mannobiose to Mannoheptaose, Specific Antigen of Pathogenic Yeast *Candida albicans*

Nobuyuki SHIBATA* and Yoshio OKAWA

Department of Infection and Host Defense, Tohoku Pharmaceutical University; 4–4–1 Komatsushima, Aoba-ku, Sendai, Miyagi 981–8558, Japan. Received January 29, 2010; accepted July 21, 2010; published online July 27, 2010

Candida albicans **contains characteristic β-1,2-linked oligomannosyl moieties in the cell wall mannan. Reduction of the reducing termini of these oligosaccharides by $NaBH_4$ causes a significant downfield shift in the NMR signals for the second and third mannose units and upfield shift of the fourth mannose unit. To show the correlation between the shift in the NMR signals and the conformations of the β-1,2-linked mannooligosaccharides, we performed molecular mechanics calculations. Six energy minima of the β-1,2-linked mannobiose were found in the relaxed map computed using the AMBER force field. Five of the six energy minima could also be generated by a simulated annealing from a 900 K molecular dynamics. Similarly, the solution conformation of the β-1,2-linked mannotriose to mannoheptaose was identified by the high temperature-simulated annealing. In the mannotetraose, the nonreducing terminal mannose unit was located near the reducing terminal one and formed a folded conformation. This result suggests that a mannose unit affects the H-1 chemical shifts of not only the second mannose unit, but also the third and fourth mannose units.**

Key words *Candida albicans*; mannan; conformation; oligosaccharide; high-temperature molecular dynamics

The antigenicity of the cells of pathogenic yeasts belonging to the genus *Candida* reside in the mannan, one of the cell wall polysaccharides. The β-1,2-linked oligomannosyl moieties, from biose to heptaose, being connected to the mannan side chain through the phosphate group, behave as the main epitope of the mannans.[1)] The β-1,2-linked oligomannosyl moieties are specifically and prominently expressed on the surface of *C. albicans*, but not on *Saccharomyces cerevisiae* and have been identified as the antigenic factor 5 of the *Candida* mannans.[2)] Candidiasis is now regarded as one of the life-threatening opportunistic infectious diseases in immunocompromised patients due to infection with the human immunodeficiency virus, tumorigenesis, treatment with immunosuppressive agents during organ transplantation, *etc.* Therefore, efforts have been made to develop serological diagnostic procedures for candidiasis by detecting either the epitope or antibody of the *C. albicans* mannans containing the β-1,2-linked oligomannosyl moieties from patients' sera.[3,4)] Several reports[5—7)] suggest the participation of the β-1,2-linked oligomannosyl moieties as the active sites of the adherence of *C. albicans* cells to mammalian cells as the initial step of the *Candida* infection. The β-1,2-linked oligomannosyl moieties bind to galectin-3,[8,9)] which is expressed in macrophages, dendritic cells, epithelial cells, *etc.* The β-1,2-linked mannooligosaccharides inhibit the adherence of the *C. albicans* cells to mouse macrophages or human intestinal Caco-2 cells.[7,10)] Furthermore, a monoclonal antibody to the β-1,2-linked oligomannosyl moieties protect the experimentally disseminated Candidiasis.[11,12)] The β-1,2-linked oligomannosyl moieties are also present in the phospholipomannan of the cell wall of *C. albicans*.[13)] Deletion of a mannosyltransferase gene, *CaMIT1*, which is responsible for the synthesis of the oligomannosyl moieties of the phospholipomannan, reduce the virulence of the *C. albicans* cells.[14)] These findings suggest that the β-1,2-linked oligomannosyl moiety has a specific structure compared to the common α-1,2-linked oligomannosyl moiety. Therefore, determination of the conformation of these oligosaccharides in an aqueous solution is very important for elucidation of the structure–activity relationship.

In some cases, the 1,2-linked oligosaccharides were shown to form specific conformations. As reported by Brant and Christ,[15)] the glycosidic torsion angles, ϕ and ψ, of the lowest energy conformer of the α-1,2-linked fucobiose form additional fucose units of higher α-1,2-linked fucooligosaccharides to self-intersect its helices. Consequently, the ϕ and ψ angles of the higher oligosaccharides differ from those of the disaccharide due to steric hindrance. The α-1,2-linked mannooligosaccharides seem to not have such a steric difficulty judging from the ϕ and ψ angles of the lowest energy conformer of the α-1,2-linked mannobiose[16,17)] and from the simple ^{1}H-NMR spectra of its higher oligosaccharides. However, the β-1,2-linked mannooligosaccharides seem to manifest a conformational property similar to the α-1,2-linked fucooligosaccharides. The assignment results of the H-1 signals of the β-1,2-linked mannooligosaccharides from biose to heptaose indicated that each intermediary mannose unit had a different chemical shift.[18)] This property is unusual for the homo-oligosaccharides of a single linkage series. Furthermore, the reduction of the reducing termini of these oligosaccharides to the corresponding alcohols caused a significant downfield shift in the H-1 signals for the second mannose unit ($\Delta\delta$=0.07—0.08 ppm) and the third mannose unit ($\Delta\delta$=0.03—0.08 ppm) and an upfield shift of the fourth mannose unit ($\Delta\delta$=0.07—0.08 ppm).[18)] For the α-1,2-linked mannooligosaccharides, a shift in the H-1 signals by the reduction mainly occurs on the second mannose unit and is shifted upfield ($\Delta\delta$=0.06—0.08 ppm) instead of downfield. Based on these results, we speculate that the reducing terminal mannose unit locates near the three units in order to affect these H-1 proton chemical shifts. Nitz *et al.*[19)] reported the conformation of the β-propyl glycoside derivatives of the β-1,2-linked mannooligosaccharides. However, the β-1,2-linked oligosaccharide moieties were connected to a phosphate group of the mannan side chains by an α-linkage. Therefore, we used the free β-1,2-linked mannooligosaccha-

* To whom correspondence should be addressed. e-mail: nshibata@tohoku-pharm.ac.jp.

rides instead of the β-propyl glycoside derivatives for the conformation analysis. The reducing terminal mannose unit of the free β-1,2-linked mannooligosaccharides mainly consists of the α-anomer.[18] The unprecedented shift effect of the H-1 chemical shift of up to the fourth carbohydrate units by treatment of these oligosaccharides with $NaBH_4$ seems to indicate a folded conformation.

The purpose of the present study is to demonstrate the close proximity between the first and the fourth mannose units by the folded conformation. To determine the lowest energy conformer of each member of the β-1,2-linked mannooligosaccharide series, we attempted application of a simulated annealing protocol from a high-temperature molecular dynamics.

Experimental

Materials The β-1,2-linked mannooligosaccharides were prepared from the mannan of the *C. albicans* NIH B-792 strain by treatment with 10 mM HCl at 100 °C for 60 min followed by gel chromatography on a Bio-Gel P-2 column.[18]

Conventions The residues of the oligosaccharides have been labeled from the reducing terminus. The glycosidic torsion angles, ϕ and ψ, are defined as H-1–C-1–O-1–C-2′ and C-1–O-1–C-2′–H-2′ (Fig. 1), respectively.

Computational Method The molecular mechanics and the molecular dynamics calculations were performed using the Insight II/Discover molecular modeling package (Biosym Technologies, San Diego, CA, U.S.A.). These calculations were performed *in vacuo* with the dielectric constant ε=80.0 using the AMBER force field with *exo*-anomeric potentials.[20] These were run on a COMTEC 4D RPC computer (Daikin Industries, Ltd., Tokyo).

Systematic Grid Search For the relaxed-body potential energy calculation of Manβ1-2Manα, the ϕ and ψ angles were stepped through 360° in increments of 5°, and, at each grid point, the internal coordinates, except for the linkage torsion angles, were fully energy minimized by 1000 cycles of the conjugate gradients. The iso-energy levels were contoured with interpolation of 1 kcal/mol above the absolute minimum.

Conformational Search by a Simulated Annealing from High-Temperature Molecular Dynamics Each β-1,2-linked mannooligosaccharide was equilibrated by running dynamics at 900 K for 20 ps. The data were collected from a subsequent 100 ps run at 900 K to generate 100 random energy structures. These structures were then separately cooled in 50 K steps, and at each step, a 1-ps molecular dynamics was performed from 500 to 300 K and then to 10 K in 10 K per 1-ps steps and finally to 5 K. Each annealing structure was then minimized using a conjugate gradient algorithm.

Molecular Dynamics Simulations The system was equilibrated using a thermal bath at 300 K for 50 ps. The data analysis was then performed for a total of 1 ns for simulation with a history output every 1000 steps.

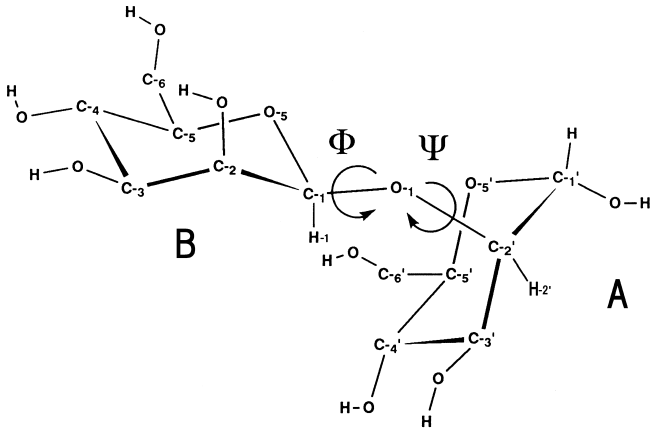

Fig. 1. Schematic Representation of Glycosidic Linkages in Manβ1-2Manα

The glycosidic linkage is described by two dihedral angles: ϕ=H-1–C-1–O-1–C-2′ and ψ=C-1–O-1–C-2′–H-2′.

Results and Discussion

Systematic Grid Search of the Lowest Energy Conformer of Manβ1-2Manα The relaxed-body potential energy map of Manβ1-2Manα was generated as shown in Fig. 2. From the iso-energy contour map, six energy minima were found with the ϕ and ψ values of (54.8, −1.2), (50.2, 177.8), (172.9, 8.6), (46.2, 150.6), (−167.8, 61.0) and (−47.8, 1.8) as listed in Table 1. The lowest energy conformer of the six minima was ϕ=54.8° and ψ=−1.2° (conformer 1). The BH1-AH1 and BH1-AH2 inter-proton distances calculated from the lowest energy conformer were 0.308 and 0.242 nm, respectively.

Conformational Search of Manβ1-2Manα by Simulated Annealing from 900 K Molecular Dynamics One-hundred generated conformers for the Manβ1-2Manα at the 900 K molecular dynamics were energy minimized by the simulated annealing protocol to give five low energy conformers, designated $SMan_2$-1 to -5 (Table 2). The ϕ and ψ angles of the lowest energy conformer, $SMan_2$-1, were 54.5° and −1.5°, respectively. The five lowest energy conformers were the same as the conformers, 1, 3, 4, 5, and 6, found from the iso-energy contour map obtained from the relaxed

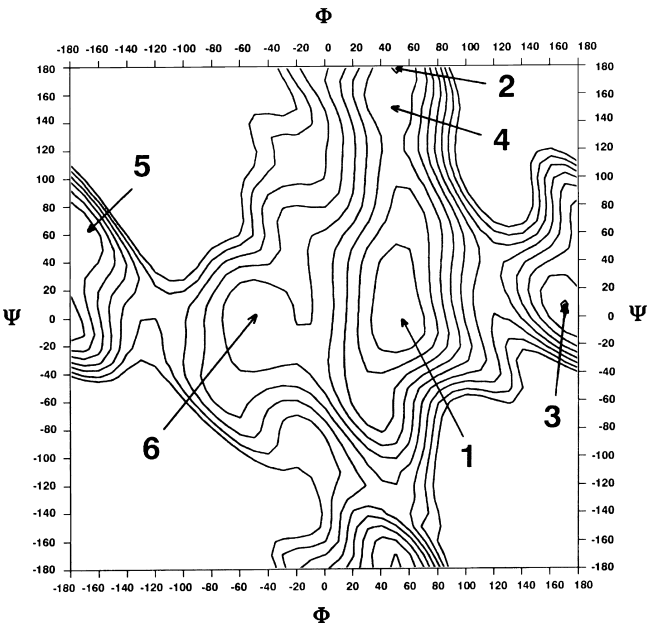

Fig. 2. Relaxed-Residue Steric Energy Map of Manβ1-2Manα as a Function of the ϕ and ψ Torsion Angles

The iso-energy contour is drawn in increments of 1 kcal/mol with respect to the absolute minimum.

Table 1. Steric Energy Minima for Relaxed-Residue Analysis of Manβ1-2Manα

Conformer	ϕ (°)	ψ (°)	ΔE (kcal/mol)	Inter-proton distance	
				BH1-AH1 (nm)	BH1-AH2 (nm)
1	54.8	−1.2	0.00	0.308	0.242
2	50.2	177.8	1.74	0.389	0.369
3	172.9	8.6	1.88	0.395	0.365
4	46.2	150.6	1.90	0.325	0.377
5	−167.8	61.0	2.97	0.386	0.376
6	−47.8	1.8	3.88	0.402	0.241

Table 2. Glycosidic Dihedral Angles and ΔE of Manβ1-2Manα

Conformer	ΔE (kcal/mol)	ϕ (°)	ψ (°)	Inter-proton distance		Corresponding conformer on relaxed map
				BH1-AH1 (nm)	BH1-AH2 (nm)	
$SMan_2$-1	0.00	54.5	−1.5	0.308	0.242	1
$SMan_2$-2	2.02	172.0	9.7	0.387	0.366	3
$SMan_2$-3	2.50	47.4	150.4	0.321	0.377	4
$SMan_2$-4	3.11	−167.3	60.8	0.385	0.375	5
$SMan_2$-5	3.92	−47.5	1.9	0.399	0.238	6

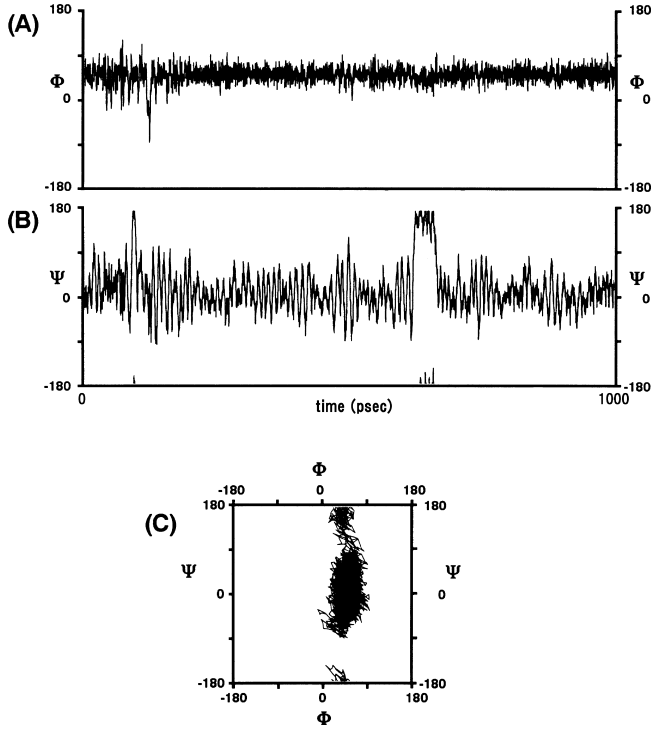

Fig. 3. Histories of the Glycosidic Torsion Angles during 1-ns Molecular Dynamics Simulations of Manβ1-2Manα *in vacuo* with the Dielectric Constant of 80.0

The molecular dynamics simulations were started with the input ϕ and ψ values corresponding to the conformer $SMan_2$-1. (A) ϕ *versus* time, (B) ψ *versus* time, (C) ϕ and ψ line graph.

map calculation of the grid search. The ϕ and ψ angles of conformer $SMan_2$-1 were used as input values for the 1-ns molecular dynamics simulation as shown in Fig. 3. The ϕ and ψ trajectories showed that the molecule dwells in a geometry characterized by the average values of ϕ=52° and ψ=7°, and that the ψ angle is more flexible than the ϕ angle. A short life time of $SMan_2$-3, the conformation of which is basically the same as conformers 2 and 4, was observed in the molecular dynamics. In keeping with this, the ϕ and ψ trajectories in a simulation started from the second lowest energy conformer, $SMan_2$-2, which corresponds to conformer 3, did not halt at the input values, and the trajectories jumped immediately to the values corresponding to the conformer $SMan_2$-1 (data not shown). Therefore, this method was also used to analyze the conformation of the β-1,2-linked mannooligosaccharides up to heptaose.

Application of Simulated Annealing from 900 K Molecular Dynamics to Conformational Search for β-1,2-Linked Mannotriose to Mannoheptaose From one-hundred generated conformers for each β-1,2-linked mannooligosaccharides, lowest energy conformers, $SMan_3$ to $SMan_7$, were obtained. The ϕ and ψ angles of these conformers are shown in Table 3. Although the ϕ angles of the second mannose unit, ϕ_{AB}, of these lowest energy conformer were similar to those of $SMan_2$-1, 49—58°, those of the third mannose unit, ϕ_{BC}, were obviously smaller, 36—38°. On the other hand, the ψ angle of the fourth mannose unit, ψ_{CD}, was greater than ψ_{AB} of $SMan_2$-1. The change in the torsion angles seems to be due to the steric effect between the first and the third and fourth mannose units. Figure 4 shows a stereodiagram of the lowest energy conformers of the β-1,2-linked mannooligosaccharides up to heptaose. For the tetraose, the reducing and non-reducing terminal mannose units, Man-A and Man-D, are closely located. Similarly, for the pentaose, Man-B and Man-E, in addition to Man-A and Man-D, are also located in the same vicinity. Because of the helical nature of the β-1,2-linked mannooligosaccharides, the heptaose also showed the proximity of the mannose units between the first and fourth units in the oligosaccharide. As shown in Fig. 4, these oligosaccharides showed the close proximity between the H-1 of Man-B and the H-1 of Man-A as well as the

Table 3. Glycosidic Dihedral Angles of β-1,2-Linked Mannooligosaccharides

Conformer	Relative total energy (kcal/mol)	Mannose residue						
		G	F	E	D	C	B	A
		ϕ_{FG} ψ_{FG} (°)	ϕ_{EF} ψ_{EF} (°)	ϕ_{DE} ψ_{DE} (°)	ϕ_{CD} ψ_{CD} (°)	ϕ_{BC} ψ_{BC} (°)	ϕ_{AB} ψ_{AB} (°)	
$SMan_2$	0.66						Manβ1-2Manα	
							54.5	
							−1.5	
$SMan_3$	−1.93					Manβ1-2	Manβ1-2Manα	
						52.3	57.2	
						25.7	−2.0	
$SMan_4$	−6.40				Manβ1-2	Manβ1-2	Manβ1-2Manα	
					48.0	37.2	48.7	
					16.8	−9.4	−11.7	
$SMan_5$	−8.62			Manβ1-2	Manβ1-2	Manβ1-2	Manβ1-2Manα	
				48.6	32.6	37.1	57.9	
				17.5	12.4	−16.8	−4.9	
$SMan_6$	−11.75		Manβ1-2	Manβ1-2	Manβ1-2	Manβ1-2	Manβ1-2Manα	
			54.6	40.9	47.9	36.4	51.9	
			29.4	−6.0	14.3	−10.8	−10.5	
$SMan_7$	−14.67	Manβ1-2	Manβ1-2	Manβ1-2	Manβ1-2	Manβ1-2	Manβ1-2Manα	
		50.8	34.8	70.8	40.6	38.4	51.3	
		24.6	−9.2	49.0	19.7	−15.1	−6.4	

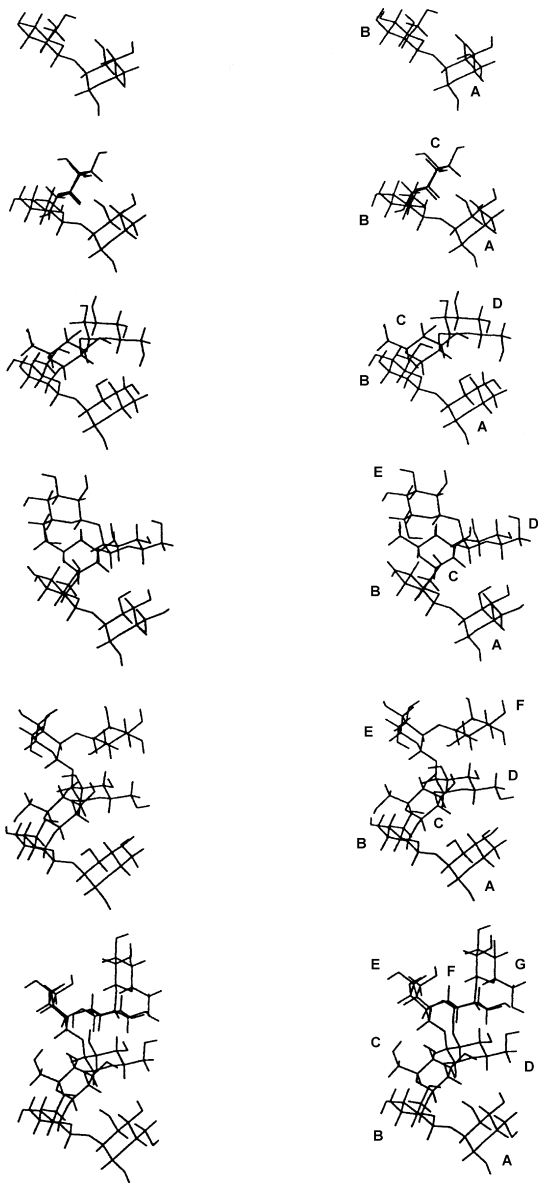

Fig. 4. Stereodiagram of the Lowest Energy Conformers of the β-1,2-Linked Mannooligosaccharides from Biose to Heptaose Obtained by Simulated Annealing from 900 K Molecular Dynamics

H-1 of Man-B and the H-2 of Man-A. This conformational nature is able to be found only by using the free oligosaccharide α-anomers. The folded conformation of the oligosaccharide series seems to provide an explanation for the characteristic shift effect of the H-1 signal of the second, third, and fourth mannose units upon reduction by treatment with $NaBH_4$ to convert the reducing terminal mannose to mannitol.[18] Similar folded conformations were reported by Breg *et al.*[21] for NeuAc (*N*-acetylneuraminic acid) α2-6Gal (galactose) β1-4GlcNAc (*N*-acetylglucosamine) and Imberty *et al.*[22] for Manα1-3Manα1-6Manβ1-4GlcNAc. The GlcNAc unit of the latter oligosaccharide affects the H-1 proton chemical shift of the α-1,3-linked mannose unit due to its steric proximity. The ϕ and ψ angles of the lowest energy conformer, $SMan_7$, were used as the input values for the 1-ns molecular dynamics simulation. As shown in Fig. 5, the ϕ and ψ trajectories oscillated as the geometry of $SMan_7$.

As pattern-recognition receptors, lectins recognize unique

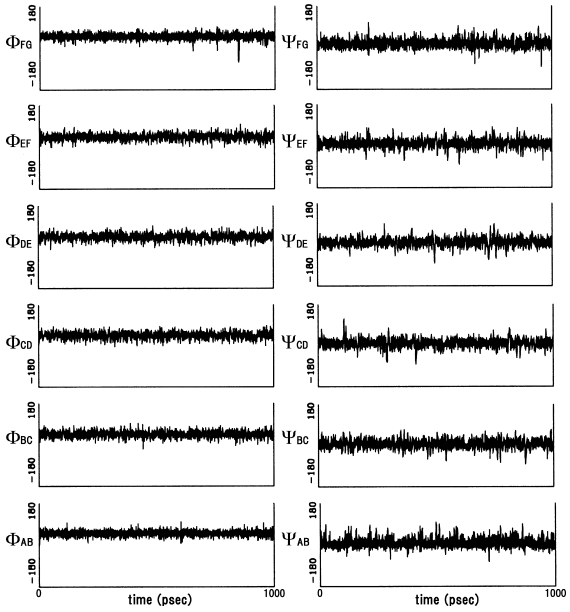

Fig. 5. Histories of the Glycosidic Torsion Angles during 1-ns Molecular Dynamics Simulations of the β-1,2-Linked Mannoheptaose *in vacuo* with the Dielectric Constant of 80.0

The molecular dynamics simulations were started with the input ϕ and ψ values corresponding to the conformer $SMan_7$.

carbohydrate ligands, or pathogen-associated molecular patterns, present on the surface of the pathogen, but absent in the host. The cell wall α-linked mannans of *C. albicans* and *S. cerevisiae* are known to bind with DC-SIGN (dendritic cell-specific intercellular adhesion molecule [ICAM]-grabbing nonintergin), dectin-2, mannan-binding protein, and mannose receptor. However, the α-linked mannose units are present in the whole organism. On the other hand, the β-1,2-linked mannose unit in the cell wall polysaccharide has a pathogen specific structure. Several studies indicate that galectin-3 specifically participates in the innate immunity, as galectin-3 is expressed in a variety of cell types including dendritic cells, macrophages, and natural killer (NK) cells, as well as activated T and B cells. Jouault *et al.*[23] reported that galectin-3 is essential for the Toll-like receptor 2-dependent cytokine production in response to the *C. albicans*, but not *S. cerevisiae*. Surprisingly, Kohatsu *et al.*[9] showed that the galectin-3 binding directly induced death of the *Candida* species containing the β-1,2-linked oligomannosyl moieties. The nature of the β-1,2-linked oligomannosyl moieties seems to be closely related to a specific conformation. Ralton *et al.*[24] reported that *Leishmania* parasites accumulate intracellular β-1,2-linked mannooligosaccharides (degree of polymerization 4—40). *Leishmania* parasites are exposed to elevated temperature when introduced into the mammalian host from the sandfly. The heat shock stress triggered the accumulation of the β-1,2-linked mannooligosaccharides which is essential for parasite differentiation and survival in the host macrophages. These results suggest that the oligosaccharide is one of the virulence factors in *Leishmania* species as well as *Candida* species, and that enzymes involved in the synthesis are potential targets for new therapies for these infections. Recently, Mille *et al.*[25] identified the β-1,2-mannosyltransferase gene family in *C. albicans*. They showed that none of these sequences contains the conserved sugar-binding region

containing the DXD (D, aspartic acid; X, any amino acid) motif (pfam Gly_transf_sug; PF04488) found in many families of glycosyltransferases. Homologs were found only in several fungal species suggesting that these enzymes form a new family of fungus-specific proteins. The unique amino acid sequence of the β-1,2-mannosyltransferase seems to correlate with the specific chemical shift of the NMR signals of the β-1,2-linked mannooligosaccharides.

References

1) Shibata N., Ichikawa T., Tojo M., Takahashi M., Ito N., Okubo Y., Suzuki S., *Arch. Biochem. Biophys.*, **243**, 338—348 (1985).
2) Shibata N., Arai M., Haga E., Kikuchi T., Najima M., Satoh T., Kobayashi H., Suzuki S., *Infect. Immun.*, **60**, 4100—4110 (1992).
3) Faille C., Michalski J. C., Strecker G., Mackenzie D. W. R., Camus D., Poulain, D., *Infect. Immun.*, **58**, 3537—3544 (1990).
4) Trinel P.-A., Faille C., Jacquinot P. M., Cailliez J.-C., Poulain D., *Infect. Immun.*, **60**, 3845—3851 (1992).
5) Li R.-K., Cutler J. E., *J. Biol. Chem.*, **268**, 18293—18299 (1993).
6) Chaffin W. L., Collins B., Marx J. N., Cole G. T., Morrow K. J. Jr., *Infect. Immun.*, **61**, 3449—3458 (1993).
7) Dalle F., Jouault T., Trinel P. A., Esnault J., Mallet J. M., d'Athis P., Poulain D., Bonnin A., *Infect. Immun.*, **71**, 7061—7068 (2003).
8) Fradin C., Poulain D., Jouault T., *Infect. Immun.*, **68**, 4391—4398 (2000).
9) Kohatsu L., Hsu D. K., Jegalian A. G., Liu F. T., Baum L. G., *J. Immunol.*, **177**, 4718—4726 (2006).
10) Fradin C., Jouault T., Mallet A., Mallet J. M., Camus D., Sinaÿ P., Poulain D., *J. Leukoc. Biol.*, **60**, 81—87 (1996).
11) Han Y., Cutler J. E., *Infect. Immun.*, **63**, 2714—2719 (1995).
12) Han Y., Kanbe T., Cherniak R., Cutler J. E., *Infect. Immun.*, **65**, 4100—4107 (1997).
13) Trinel P. A., Plancke Y., Gerold P., Jouault T., Delplace F., Schwarz R. T., Strecker G., Poulain D., *J. Biol. Chem.*, **274**, 30520—30526 (1999).
14) Mille C., Janbon G., Delplace F., Ibata-Ombetta S., Gaillardin C., Strecker G., Jouault T., Trinel P. A., Poulain D., *J. Biol. Chem.*, **279**, 47952—47960 (2004).
15) Brant D. A., Christ M. D., "Computer Modeling of Carbohydrate Molecules," ed. by French A. D., Brady J. W., ACS Symposium Series 430, American Chemical Society, Washington, DC., 1990, pp. 42—68.
16) Homans S. W., Pastore A., Dwek R. A., Rademacher T. W., *Biochemistry*, **26**, 6649—6655 (1987).
17) Edge C. J., Singh U. C., Bazzo R., Taylor G. L., Dwek R. A., Rademacher T. W., *Biochemistry*, **29**, 1971—1974 (1990).
18) Shibata N., Hisamichi K., Kikuchi T., Kobayashi H., Suzuki, S., *Biochemistry*, **31**, 5680—5686 (1992).
19) Nitz M., Ling C. C., Otter A., Cutler J. E., Bundle D. R., *J. Biol. Chem.*, **277**, 3440—3446 (2002).
20) Homans S. W., *Biochemistry*, **29**, 9110—9118 (1990).
21) Breg J., Kroon-Batenburg L. M. J., Strecker G., Montreuil J., Vliegenthart J. F. G., *Eur. J. Biochem.*, **178**, 727—739 (1989).
22) Imberty A., Perez S., Hricovini M., Shah R. N., Carver J. P., *Int. J. Biol. Macromol.*, **15**, 17—23 (1994).
23) Jouault T., El Abed-El Behi M., Martínez-Esparza M., Breuilh L., Trinel P. A., Chamaillard M., Trottein F., Poulain D., *J. Immunol.*, **177**, 4679—4687 (2006).
24) Ralton J. E., Naderer T., Piraino H. L., Bashtannyk T. A., Callaghan J. M., McConville M. J., *J. Biol. Chem.*, **278**, 40757—40763 (2003).
25) Mille C., Bobrowicz P., Trinel P. A., Li H., Maes E., Guerardel Y., Fradin C., Martínez-Esparza M., Davidson R. C., Janbon G., Poulain D., Wildt S., *J. Biol. Chem.*, **283**, 9724—9736 (2008).